Duffing oscillators: Control and memory effects

Adriano A. Batista,[1] F. A. Oliveira,[2] and H. N. Nazareno[2]
[1]*Departamento de Física, Universidade Federal de Campina Grande, Campina Grande, Paraíba, 58109-970, Brazil*
[2]*Instituto de Física and International Center of Condensed Matter Physics, Universidade de Brasília, Caixa Postal, 04455, Brasília, DF 70919-970, Brazil*

(Received 14 January 2007; revised manuscript received 19 March 2008; published 23 June 2008)

In the first part of this article we study the hysteretic bistable response of Duffing oscillators and show ways to control the switching between stable branches of this nonlinear response. The control mechanism is either applied through a pulse that can be in phase or out of phase with the periodic driving force or through a frequency-modulated driving force. In the second part we show how memory effects in dissipation qualitatively and quantitatively alter the dynamics of Duffing oscillators. We show how memory functions corresponding to different dissipative regimes (diffusion, subdiffusion, and superdiffusion) affect the oscillator. In particular, we obtain universal power laws for the absoption when the driving frequency $\omega \to 0$. For subdiffusive memories the power law exponents $\nu < 2$, for diffusive memories $\nu = 2$, and for superdiffusive memories $\nu > 2$.

DOI: 10.1103/PhysRevE.77.066216 PACS number(s): 05.45.−a, 05.40.Jc, 07.05.Dz, 85.85.+j

I. INTRODUCTION

Duffing oscillators, along with the van der Pol oscillator, Lorenz equations, and the logistic map, have been one of the mostly studied nonlinear dynamical systems [1–3]. A number of systems are modeled by the Duffing equation, such as analog circuits [4], a relativistic electron in a magnetic field [5], the current biased Josephson junction [6], and microelectromechanical systems (MEMS) or nanoelectromechanical systems (NEMS) [7]. Recently, experimental development of MEMS and NEMS have spurred new interest in Duffing oscillators. The dynamics of the fundamental mode of doubly clamped mechanical resonators is well approximated by the Duffing equation. Furthermore, these micromechanical devices exhibit a bistable response quantitatively similar to the one obtained in Duffing oscillators [8]. Since only a relatively small force is needed for driving these systems into the nonlinear regime, there is a wide range of applications such as frequency mixing [9], synchronization [10], bistable response, and amplification using bifurcation points [11], that are accessible to experimental investigation.

Here we will study some aspects of Duffing oscillators that we think have technological applications for MEMS and NEMS and basic scientific interest as well. On the technological side we propose two simple control mechanisms to switch between the stable branches of the bistable hysteretic response of ac-driven Duffing oscillators. The first control mechanism is a force pulse whose center frequency is equal to the frequency of the ac driving force of the oscillator. The pulses can be in or out of phase with the ac driving force depending on which branch of the bistable response the oscillator is initially. The second control mechanism is based on frequency modulation of the ac driving force. On the more scientific side, we propose to study phenomena related to non-Markovian dissipation (i.e., dissipation with memory) using a Duffing oscillator as a probe. In one simple experiment it is possible to detect the presence of memory effects and quantitatively measure the memory function. In this experiment a spherical Brownian particle is attached to the middle of a doubly clamped resonator or to the free end of a carbon nanotube, where the amplitude of the oscillation is highest. The calculated memory thus obtained would be very similar to the one of the free Brownian particle, because the size of this particle is of the order of hundreds of nms while the width of a NEMS resonator beam is typically of the order of a few nms. Such experimental measurement of the memory function could provide a better understanding of Brownian motion, since a determination of the memory function will tell us what kind of random motion the free Brownian particle will have: subdiffusive, diffusive, or superdiffusive [12].

Nonlinear equations with non-Markovian dissipation, such as the Duffing oscillator equation, is a natural outgrowth of the generalized Langevin equation. In such systems the memory of non-Markovian dissipative processes arises from the weak coupling of the oscillator with a thermal heat bath of harmonic oscillators once the heat bath degrees of freedom are integrated out [13]. Memory effects will become more and more relevant as micromechanical devices become smaller and smaller, since the natural frequency of these resonators gets larger. Recently, carbon nanotube-based NEMS [14] were developed whose fundamental mode is in the GHz region at room temperature and pressure conditions, a huge development over earlier MEMS that operated in kHz. In such a high-frequency device there could be memory effects in the coupling between the oscillating beam and the air surrounding it in a manner similar to what happens to a fast moving sphere in a simple fluid [15]. Furthermore, if the nonlinear oscillator we are modeling is an atomic force microscope in tapping mode over a biological system, we may have an adhesion problem and that will become a non-Markovian dissipative process at high frequencies. Yet another application of NEMS in which memory effects can become relevant is when an atomic force microscope microcantilever is submerged in a liquid environment, such as in the recent experiment of Kim and Kihm [16].

Harmonic excitations of viscoelastic nonlinear bars with equations similar to our Duffing equations with non-Markovian dissipation have been studied numerically by

Suire *et al.* [17]. They did not study though the bistable response and their model includes a cubic nonlinear term in the dissipation, which is of higher order in the perturbative approximation and can, for weakly nonlinear systems, be safely neglected.

It is important to note that mathematically an oscillator with Markovian dissipation is qualitatively different from an oscillator with non-Markovian dissipation. In the first case we have an ordinary differential equation (ODE) system, while in the latter one we have an integrodifferential equation, which in general can be rewritten in the form of an ODE system of infinite dimensionality. We said "in general" because in special cases, such as when the memory function is a decaying exponential, the memory adds only one extra dimension to the ODE system. We will show in this article that for each new time scale in the dissipation process we introduce a new dimension into the dynamical system. To analyze the importance of memory effects in the dissipation mechanism we obtain absorption curves for the oscillator, each one for a different kind of memory function (i.e., subdiffusive, diffusive, or superdiffusive memories).

In this article we will analyze the ac response of our nonlinear Duffing oscillator using the averaging method (AM), which is generally used to eliminate explicit time dependence of periodically driven ODE systems. A survey of the theory of averaging and many other results can be found in Refs. [1,18].

In Sec. II we describe the nonlinear bistable response of Duffing oscillators with simple Markovian dissipation. This section is included with the objective of describing the background and setting the stage for the subsequent study of the non-Markovian oscillator. In Sec. III we introduce the driven Duffing oscillator with non-Markovian dissipation and correlated noise. We show that when the random force is much smaller than the external driving force, in general (away from bifurcation points) the random force can be neglected from the equations of motion of the oscillator. We investigate the oscillator in three different dissipation regimes (subdiffusion, diffusion, and superdiffusion) by studying the linear and nonlinear responses of the Duffing oscillator to either an initial excitation, such as a δ function, or to an ac-driving force. In Sec. IV we discuss the numerical results. This section is divided in two subsections: one for Duffing oscillators with Markovian dissipation and the other for non-Markovian dissipation. In the first subsection we map the bistable region as a function of the driving force amplitude and frequency and apply the control methods for switching between stable branches of the bistable response. In the second subsection we obtain general results on the absorption power for the non-Markovian oscillator in the three regimes of dissipation through either δ-driven or ac-driven responses. Finally in Sec. V we draw our conclusions.

II. THE DUFFING OSCILLATOR

In this section we describe the prior art concerning nonlinear bistable response in Duffing oscillators in order to make the article more readable and self-contained. For further details please see Refs. [2,19].

The forced Duffing equation with Markovian dissipation in dimensionless format is given by

$$\ddot{x} + \omega_0^2 x = -\gamma\dot{x} - \alpha x^3 + F_0 \cos \omega t, \tag{1}$$

in which γ, α, and $F_0 \sim O(\epsilon)$, where $\epsilon \ll 1$. Since we want to apply the AM to situations in which we have detuning it is convenient to rewrite Eq. (1) in a more appropriate form with the notation $\Omega = \omega_0^2 - \omega^2$, where we also have $\Omega \sim O(\epsilon)$. With the substitution we obtain

$$\ddot{x} + \omega^2 x = -\Omega x - \gamma\dot{x} - \alpha x^3 + F_0 \cos \omega t. \tag{2}$$

We can rewrite Eq. (2) in the form

$$\dot{x} = y, \quad \dot{y} = -\omega^2 x + f(x,y,t),$$

where $f(x,y,t) = -\Omega x + F_0 \cos \omega t - \gamma y - \alpha x^3$. We now set the above equation in slowly varying form with the Van der Pol transformation

$$\begin{pmatrix} x \\ y \end{pmatrix} = \begin{pmatrix} \cos \omega t & -\sin \omega t \\ -\omega \sin \omega t & -\omega \cos \omega t \end{pmatrix} \begin{pmatrix} u \\ v \end{pmatrix}$$

and obtain

$$\begin{pmatrix} \dot{u} \\ \dot{v} \end{pmatrix} = \begin{pmatrix} \cos \omega t & -\frac{1}{\omega}\sin \omega t \\ -\sin \omega t & -\frac{1}{\omega}\cos \omega t \end{pmatrix} \begin{pmatrix} 0 \\ f(x,y,t) \end{pmatrix}.$$

After averaging we find

$$\dot{u} = \frac{-1}{2\omega}\left[\Omega v + \gamma\omega u + \frac{3\alpha}{4}(u^2 + v^2)v\right],$$

$$\dot{v} = \frac{-1}{2\omega}\left[-\Omega u + F_0 + \gamma\omega v - \frac{3\alpha}{4}(u^2 + v^2)u\right]. \tag{3}$$

The fixed points of the above equation can be found by solving the following cubic in r^2:

$$r^2[(\Omega + 3\alpha r^2)^2 + \gamma^2\omega^2] = F_0^2/4, \tag{4}$$

where $u = 2r \cos \theta$ and $v = 2r \sin \theta$. From the above equations we find that the necessary conditions for the existence of three real roots is $\alpha \neq 0$ and $\Omega^2 - 3\gamma^2\omega^2 > 0$, or $|\Omega| > \sqrt{3}\gamma\omega$ (i.e., $|\omega^2 - \omega_0^2| > \sqrt{3}\gamma\omega$). The angle θ can be found from

$$\sin \theta = -\frac{2\gamma\omega r}{F_0}.$$

The average power absorbed per period of drive by the Duffing oscillator is given by

$$\bar{P} = -\frac{\omega v F_0}{2} = 2\gamma\omega^2 r^2$$

$$= \frac{F_0^2 \gamma\omega^2}{2[(\Omega + 3\alpha r^2)^2 + \gamma^2\omega^2]}$$

$$\approx \frac{F_0^2 \gamma\omega^2}{2\left[\left(\Omega + 3\alpha \frac{F_0^2}{4[\Omega^2 + \gamma^2\omega^2]}\right)^2 + \gamma^2\omega^2\right]}.$$

Control over the bistability region can be performed by the

action of designed control pulses with the help of the AM through Eq. (4). We notice that we can use pulses in phase or out of phase with the driving field. The choice will depend on which branch of the bistable region the oscillator is. Equation (4) also shows that a driving field with a frequency modulation can also act as a control switch. In the case of a driving force given by $F(t)=F_0\cos(\omega t+\beta/\nu\cos\nu t)$ or $F(t)=F_0\cos(\omega t+\beta/\nu\sin\nu t)$, we could have, for special values of β and ν, a hysteresis loop around the bistable region, in a manner similar to what is done with ferromagnetic materials. The looping direction will depend on the value of parameters of the Duffing oscillator.

III. DUFFING OSCILLATOR WITH MEMORY

The driven Duffing equation with non-Markovian dissipation and correlated noise is given by the following equation:

$$\ddot{y}=-\int_{-\infty}^{t}\Gamma(t-t')\dot{y}(t')dt'-\omega_0^2y-\alpha y^3+F(t)+R(t), \quad (5)$$

where the nonrandom driving force can be $F(t)=K_0e^{-i\omega t}+K_0^*e^{i\omega t}$ or $F(t)=\delta(t)$. Such equations of motion are obtained when our Duffing oscillator is coupled to a harmonic thermal reservoir. Here $R(t)$ is a random force, whose time correlation is given by $\langle R(t)R(t')\rangle=T\Gamma(t-t')$, where T is the temperature and $\Gamma(t)$ is a memory function obtained from integrating out the reservoir degrees of freedom [13]. In what follows we assume the thermal noise is not very strong and that we are not close to a bifurcation point. We then perform a linear analysis of Eq. (5) by taking the noise term as a perturbation, since we consider $R(t)\ll K_0$. We have $y(t)=x(t)+\delta y(t)$, where $x(t)$ is a stable solution of Eq. (5) when $R(t)=0$ and $\delta y(t)$ is the perturbation response. We then find the equation for the linear response

$$\delta\ddot{y}=-\omega_0^2\delta y-\int_{-\infty}^{t}dt'\,\gamma(t-t')\delta\dot{y}(t')-3\alpha x(t)^2\delta y+R(t). \quad (6)$$

Since this equation is linear we can take a statistical average and eliminate $R(t)$. We then obtain an equation for $z(t)=\langle\delta y\rangle$, where the angles indicate the statistical average. This averaged equation is

$$\ddot{z}+[\omega_0^2+3\alpha x(t)^2]z=-\int_{-\infty}^{t}dt'\,\gamma(t-t')\dot{z}(t'). \quad (7)$$

When $F(t)$ is periodic $x(t)$ is a stable periodic orbit, hence, we realize that this equation represents a parametrically driven oscillator with dissipation, only different from the usual parametric oscillator due to the non-Markovian character of the dissipation. This parametric oscillator may present the regions of instability, known as Arnold tongues, of the generic parametric oscillator given by Hill's equation [20]. Consequently, the question of whether the noise will considerably affect the dynamics of the driven Duffing oscillator depends on the oscillator being inside or outside of the Arnold tongues. If the oscillator is inside the Arnold tongue the solution $z=0$ is unstable and therefore we cannot neglect the effects of noise. Otherwise, the solution $z=0$ is stable and we can neglect the effects of noise, provided we are not close to a bifurcation point as we assumed initially. The strongest parametric instability occurs when the driving frequency ω is near the renormalized natural frequency of Eq. (7), since $x(t)$ is squared. Once dissipation is present this instability requires a minimum amplitude of the driving force to occur and this threshold becomes higher and higher for lower and lower parametric resonances as can be seen in Ref. [20]. Further below we show numerical results on these zones of instability. Basically, we find out that noise does not affect the equations of motion of the Duffing oscillator when the driving force is not large and the driving frequency is small. When $F(t)=\delta(t)$, we find numerically that, for random initial values of $z(0)$ and $\dot{z}(0)$ using the Gibbs probability distribution or any other symmetric probability distribution, the $z(t)$ cancel out when summed. Hence, we neglect $R(t)$ in the dynamics of the Duffing oscillator and obtain

$$\ddot{x}=-\int_{-\infty}^{t}\Gamma(t-t')\dot{x}(t')dt'-\omega_0^2x-\alpha x^3+F(t). \quad (8)$$

A linear analysis of the above equation shows us that the non-Markovian oscillator has some qualitative differences from the usual damped oscillator. For instance, when ac driven, the resonant frequency of the non-Markovian oscillator is generally shifted from ω_0 while the usual oscillator always has the resonant frequency given by ω_0. When the non-Markovian oscillator is driven by an impulsive force, the frequency of the decaying transient oscillations can be blue shifted in comparison with ω_0, while for the usual damped oscillator the oscillations are always redshifted. The solution of the above equation when $\alpha=0$ and the drive is $F(t)=\delta(t)$ is given by

$$x(t)=\frac{1}{2\pi}\int_{-\infty}^{\infty}\frac{e^{-i\omega t}d\omega}{\Omega-i\omega\tilde{\Gamma}(i\omega)}, \quad (9)$$

where $\tilde{\Gamma}(i\omega)$ is the Laplace transform of the memory function. When $\alpha>0$ we have

$$x_\omega=x_\omega^0-\frac{\alpha}{(2\pi)^2}x_\omega^0\int_{-\infty}^{\infty}x(t)^3e^{-i\omega t}dt$$

$$=x_\omega^0-\frac{\alpha}{(2\pi)^2}x_\omega^0\int_{-\infty}^{\infty}d\omega_1x_{\omega_1}\int_{-\infty}^{\infty}d\omega_2x_{\omega_2}x_{\omega-\omega_1-\omega_2}, \quad (10)$$

where

$$x_\omega^0=\frac{1}{\Omega-i\omega\tilde{\Gamma}(i\omega)}.$$

The simple fact that the Fourier transform of $x(t)$ is related to the memory function could be used to verify experimentally to what extent the dynamics of the NEMS is non-Markovian. Furthermore, with this information, one could, in principle, accurately measure the memory function. A determination of the memory function will tell us what kind of random motion the free Brownian particle will have: subdiffusive, diffusive, or superdiffusive [12]. Although nanoscale displacement de-

tection in NEMS is a highly challenging task, it has been recently accomplished by Almog *et al.* [11] and also by Peng *et al.* [14]. Another approach to determine the memory function is through the measurement of the amplitude and phase of the steady-state response $x(t)=a\cos(\omega t+\varphi)$ for a frequency range around the resonance of the non-Markovian Duffing oscillator to an ac driving force.

At steady state we look for a solution of the form $x(t)=x_\omega e^{-i\omega t}+x_\omega^* e^{i\omega t}$, which is the first term of a perturbation series expansion of the true periodic solution. With this substitution in Eq. (8) we find

$$[\Omega - i\omega\tilde{\Gamma}(i\omega) + 3\alpha|x_\omega|^2]x_\omega = K_0. \tag{11}$$

We simplify the above equation with the shorthand notation $r^2=|x_\omega|^2$ and $z(\omega)=\Omega-i\omega\tilde{\Gamma}(i\omega)$. Hence we obtain

$$[z(\omega)+3\alpha r^2]r^2 = K_0 x_\omega^*,$$

which can be simplified to

$$|z(\omega)+3\alpha r^2|r = |K_0|. \tag{12}$$

The above development was a simple application of straightforward perturbation expansion. In the following we proceed to investigate the Duffing equation with memory using the AM, which allows us to study the stability of periodic orbits. In the slowly varying frame we have

$$\begin{pmatrix}\dot{u}\\ \dot{v}\end{pmatrix} = \begin{pmatrix} -\cos\omega t & \frac{1}{\omega}\sin\omega t \\ \sin\omega t & \frac{1}{\omega}\cos\omega t\end{pmatrix}\begin{pmatrix}0\\ -f(x,y,t)\end{pmatrix} = \frac{-1}{\omega}\begin{pmatrix}\sin\omega t f(x,y,t)\\ \cos\omega t f(x,y,t)\end{pmatrix},$$

where now $f(x,y,t)=-\int_{-\infty}^{t}\Gamma(t-t')y(t')dt'-\alpha x^3+K_0e^{-i\omega t}+K_0^*e^{i\omega t}$. After averaging we obtain

$$\dot{u} = -\frac{1}{2\omega}\left\{\Omega v+\omega[u\ \mathrm{Re}\ \tilde{\Gamma}(i\omega)-v\ \mathrm{Im}\ \tilde{\Gamma}(i\omega)] + \frac{3\alpha}{4}(u^2+v^2)v+2\ \mathrm{Im}\ K_0\right\},$$

$$\dot{v} = -\frac{1}{2\omega}\left\{-\Omega u+\omega[u\ \mathrm{Im}\ \tilde{\Gamma}(i\omega)+v\ \mathrm{Re}\ \tilde{\Gamma}(i\omega)] - \frac{3\alpha}{4}(u^2+v^2)u+2\ \mathrm{Re}\ K_0\right\}. \tag{13}$$

The average power absorbed by this viscoelastic nonlinear oscillator is given by

$$\bar{P}(\omega) = -\omega[K_0(\bar{v}-i\bar{u})+\mathrm{c.c.}]/2 = \frac{2|K_0|^2\omega^2\ \mathrm{Re}\ \tilde{\Gamma}(i\omega)}{|z(\omega)+3\alpha r^2|^2} \approx \frac{2|K_0|^2\omega^2\ \mathrm{Re}\ \tilde{\Gamma}(i\omega)}{\left|z(\omega)+3\alpha\frac{|K_0|^2}{|z(\omega)|^2}\right|^2}, \tag{14}$$

where $\bar{u}$ and $\bar{v}$, are the fixed points of Eq. (13).

We will next analyze the three different regimes of non-Markovian dissipation: diffusive, subdiffusive, and superdiffusive. In what follows, we choose for each dissipative mechanism a representative memory function. Each dissipative regime will have its own universal response (power law in the absorption function) in the limit the driving frequency $\omega\to 0$. In principle this limit could be probed with an oscillator with small elastic constant.

A. Diffusive memory

In general, it is difficult to numerically integrate Eq. (8) for a generic memory function, but in the special case the memory is an exponential function $\Gamma(t)=\Gamma_0 e^{-t/\tau}$, there is a simple method in which the integrodifferential Eq. (8) becomes an ODE system of dimension 3. By setting $z(t)=\int_{-\infty}^{t}\Gamma(t-t')\dot{x}(t')dt'$, we find the ODE system

$$\ddot{x} = -z-\omega_0^2 x-\alpha x^3+F(t), \quad \dot{z}=\Gamma_0\dot{x}-z/\tau, \tag{15}$$

which was numerically integrated with the initial values given by $x(0)=z(0)=0$ and $\dot{x}(0)=0$ when $F(t)=K_0e^{-i\omega t}+K_0^*e^{i\omega t}$, or $x(0)=z(0)=0$ and $\dot{x}(0)=1$ when $F(t)=\delta(t)$. The main advantage of this transformation from an integrodifferential equation into an ODE system is that we can use off-the-shelf integration algorithms such as the Runge-Kutta algorithm to integrate the ODE system, what cannot be done in general for the integrodifferential equation in Eq. (8). The Laplace transform of the exponential memory is given by $\tilde{\Gamma}(i\omega)=\Gamma_0(1/\tau+i\omega)/(1/\tau^2+\omega^2)$. This memory function always leads to diffusive processes for a free Brownian particle since $(0<\tilde{\Gamma}(0)<\infty)$ [12]. It also implies in the blue-shifted resonant frequency obtained from the continued fraction expansion of

$$\omega_R^2 = \frac{\omega_0^2}{1-\frac{\Gamma_0}{1/\tau^2+\omega_R^2}},$$

which can be rewritten as

$$\omega_R^2 = \omega_0^2+\frac{\Gamma_0}{1+1/(\tau\omega_R)^2} \tag{16}$$

for clarity. Note that if we had two time scales in the dissipation process, e.g., $\Gamma(t)=\Gamma_0e^{-t/\tau_0}+\Gamma_1e^{-t/\tau_1}$ we would have two more dimensions in the ODE system than in the Markovian oscillator. In general, a memory function can be written as $\Gamma(t)=\Sigma_i\Gamma_i e^{-t/\tau_i}$, in which the more terms in the summation (leading in the continuous limit to a Laplace transform) the more dimensions in the ODE system. Implying also in more extensive changes in the dynamics of the oscillator under study. The average power absorbed in diffusive dissipation near $\omega=0$ is given by $\lim_{\omega\to 0}P(\omega)\propto\omega^2$. This is a universal power law for oscillators with diffusive memory. This result is independent of the specific memory function used or of nonlinear effects according to Eq. (14).

B. Subdiffusive memory

We choose the representative memory $\Gamma(t)=\frac{\Gamma_0}{\sqrt{t}}$ of subdiffusive processes $[\tilde{\Gamma}(0)\to\infty]$ from Ref. [12]. It has the

Laplace transform $\tilde{\Gamma}(i\omega)=\Gamma_0\sqrt{\frac{\pi}{2|\omega|}}[1+i\ \mathrm{sgn}(\omega)]$. We also find that subdiffusivity also implies in a blueshift of the resonant frequency. The equation for the resonant frequency ω_R in the linear regime is given by

$$\omega_R^2=\omega_0^2+\Gamma_0\sqrt{\pi\omega_R/2}. \tag{17}$$

The average power absorbed near $\omega=0$ is given by $\lim_{\omega\to 0} P(\omega)\propto\omega^{3/2}$. Although, the exact exponent of the absorption may vary for different subdiffusive processes, this exponent has to be less than 2 for all subdiffusive processes [assuming $\lim_{\omega\to 0}\tilde{\Gamma}(i\omega)\propto\omega^{-\nu}$, where $\nu>0$].

C. Superdiffusive memory

We choose the representative memory function for superdiffusive processes $[\tilde{\Gamma}(0)\to 0]$ to be $\Gamma(t)=\Gamma_0 e^{-t/\tau_0}-\Gamma_1 e^{-t/\tau_1}$, in such a way that $\Gamma_0\tau_0=\Gamma_1\tau_1$. It has the following Laplace transform:

$$\tilde{\Gamma}(i\omega)=\Gamma_0\frac{1/\tau_0+i\omega}{1/\tau_0^2+\omega^2}-\Gamma_1\frac{1/\tau_1+i\omega}{1/\tau_1^2+\omega^2},$$

where we choose $\Gamma_0>\Gamma_1$ and $\tau_0<\tau_1$. The resonant frequency in the linear regime is given implicitly by

$$\omega_R^2\left[1-\frac{\Gamma_0}{1/\tau_0^2+\omega^2}+\frac{\Gamma_1}{1/\tau_1^2+\omega^2}\right]=\omega_0^2. \tag{18}$$

The advantage of this superdiffusive memory over others is that it allows for easy numerical integration of the equations of motion (8) of the Duffing oscillator. The average power absorbed near $\omega=0$ is given by $\lim_{\omega\to 0} P(\omega)\propto\omega^4$. In general the exponent of the absorption for superdiffusive processes goes as ω^ν for $\omega\to 0$, where $\nu>2$.

IV. NUMERICAL RESULTS

We now characterize the bistable regime of the Duffing oscillators and present the response of these oscillators to appropriately designed pulses that act as a switch between the stable branches of this bistable regime. The equations of motion were integrated using the fourth-order Runge-Kutta algorithm with 2048 steps per cycle of drive. Furthermore, we investigate the effects of the three different kinds of non-Markovian dissipation on the response of the oscillator to either a δ-function excitation or to an ac drive at steady state. In the case of an exponentially decaying memory (diffusive process) we can easily integrate the equations of motion both for the linear and nonlinear regimes. On the other hand, we only study the linear responses when the memory is subdiffusive or superdiffusive due difficulties in integrating nonlinear integrodifferential equations.

A. Markovian dissipation

In the bistable region of the ac-driven Duffing oscillator we have three periodic orbits, from which two are stable, with the unstable orbit in between the two stable ones. The smaller orbit, on average, absorbs less energy from the driving field than the larger one. This is due to one branch being nearly in phase with the driving field, while the other nearly out of phase. The time series of $\dot{x}(t)$ corresponding to the two stable branches of the bistable region are shown in Fig. 1, in frames (a) and (c), alongside with the corresponding Fourier transforms in frames (b) and (d). One can see in the figure a difference in amplitude of the third harmonic between the two responses around two orders of magnitude. That difference could in principle be used for designing microwave modulators where the source of radiation is a charged vibrating MEMS or NEMS. In one of the branches we would have a high signal at the third harmonic, the on state, or bit 1, while at the other branch we would have a small signal that could represent the off state, or bit 0.

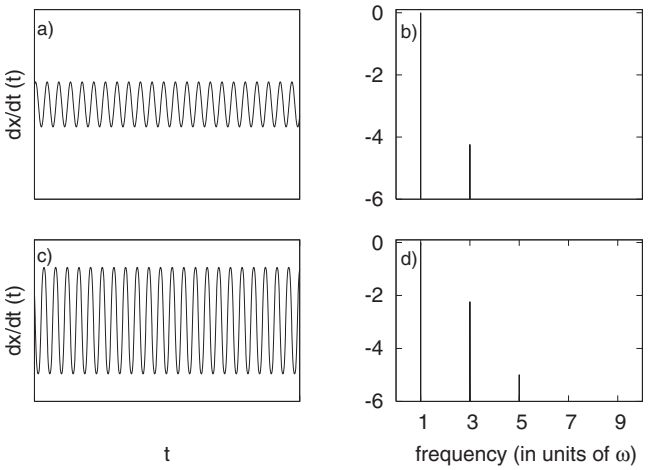

FIG. 1. Example of two stable responses of the Duffing oscillator at bistability with the corresponding Fourier transforms. The parameters are given by $\omega_0=1.0$, $\omega=1.43$, $\alpha=1.0$, $\gamma=0.2$, and $F_0=0.40$.

A hysteretic loop of the absorption line as a function of the drive amplitude is shown in Fig. 2. We plot together the results from numerical integration of Eq. (1) and also from the AM of Eq. (4). We note that the accuracy of the AM is

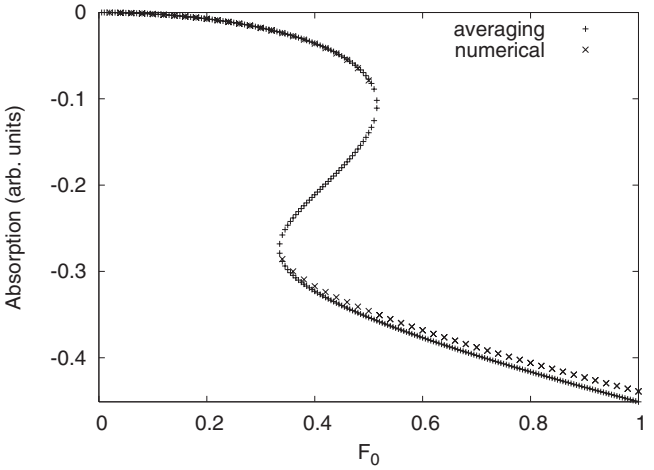

FIG. 2. Hysteresis region. Only the stable branches are shown in the numerical absorption curve, while the AM theoretical curve shows all three branches. The parameters are given by $\omega_0=1.0$, $\omega=1.43$, $\alpha=1.0$, and $\gamma=0.2$.

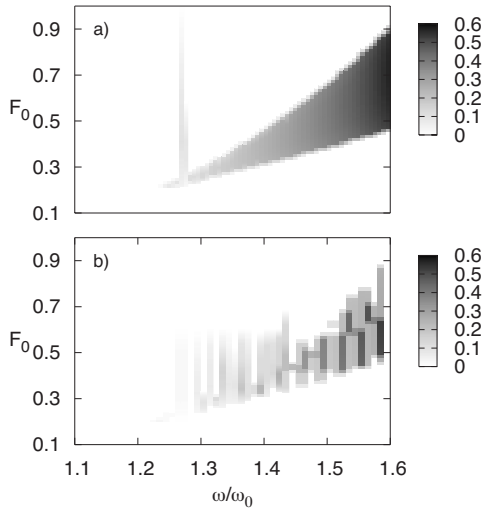

FIG. 3. Bistability region as a function of driving force amplitude and the ratio driving frequency and natural frequency of the oscillator. Darker areas indicate larger differences in absorption between the stable branches of the bistable response. (a) Analytical results based on Eq. (4). (b) Full numerical results of bistability region as a function of driving force amplitude and the ratio driving frequency and natural frequency of the oscillator. For these results Eq. (1) was numerically integrated. The parameters are given by $\omega_0=1.0$, $\alpha=1.0$, and $\gamma=0.2$.

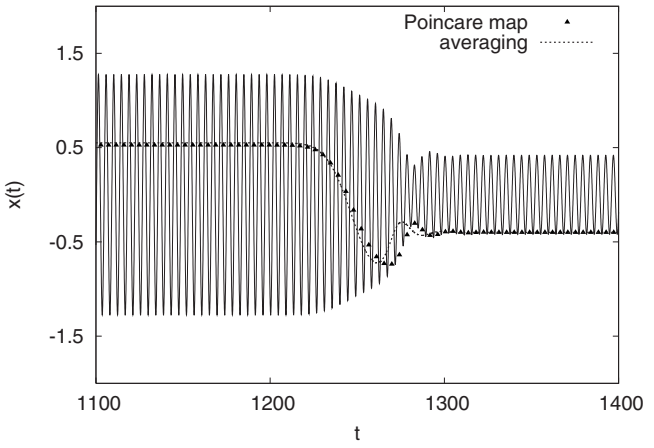

FIG. 4. Time evolution of $x(t)$ for the Duffing oscillator subjected to an ac drive and a control pulse (with a Gaussian-shaped envelope) is shown by the thin line plot. Here the control field is out of phase by π with the driving field. The dotted line is obtained from integrating the corresponding averaged system of equations. The triangles represent the Poincaré map of the full numerical solution; its close proximity with the AM results shows that the AM is quite accurate in predicting the behavior of the Duffing oscillator under the action of an adiabatic pulse. The peak height of the control pulse is 0.127, the width is 17.6, and the median is at $t=1248$. The parameters of the oscillator are $\omega_0=1.0$, $\omega=1.43$, $\alpha=1.0$, $\gamma=0.2$, and $F_0=0.40$.

better for smaller amplitudes of the driving force, which is in accordance to what we expected since this is a perturbative method. In this case one could also observe bistability by varying the drive frequency if the amplitude of the driving force is in the interval between 0.3 and 0.5. One can see this in Fig. 3, where we show the bistability region of the Duffing oscillator given as a function of driving frequency and driving field amplitude. These results are based on the AM results of Eq. (4). One needs considerable blueshifted detuning to start seeing the bistability response. We verify the global extension of the applicability of the AM by comparing the results of Fig. 3(a) with those of Fig. 3(b), which displays the bistability region of the Duffing oscillator obtained from the numerical integration of Eq. (1). We obtain a fairly good agreement with the previous result given by AM calculations, indicating that the AM is a very good predictor of the bistable behavior of Duffing oscillators.

These results showing the bistable response will serve us as a guide for constructing the control switch between the stable modes. The AM calculation tells us what is the necessary minimum amplitude for the pulse in order to realize the switch. If the system is initially in the smaller orbit we then need an in-phase pulse to reach the jump point and then the other branch, and vice versa, if we are in the larger orbit we need an out-of-phase pulse. At the jump points we have an abrupt change both in the amplitude and in the phase of the oscillation. Although the pulse is adiabatic the transition at the jump points will be abrupt, hence the need for the peak field of the pulse be large enough to take the Duffing oscillator out of the bistable region in order to accomplish the transition with certainty.

We can see the effects of a control pulse acting on the driven Duffing oscillator in Fig. 4. In this figure we present the time evolution of $x(t)$, where the time evolution is given through the full numerical integration (the oscillating line), the Poincaré map (triangles), and its approximation by the AM calculation (dotted line). Here the pulse is out of phase with respect to the driving force, hence from looking at Fig. 2 we conclude that the oscillator is initially in the lower branch and, as the pulse amplitude grows, we nearly adiabatically go down along the lower branch until the jump point is reached. At this moment we swing to the other branch and stay there. After the jump, the high odds of staying in the smaller branch are due to the pulse being fairly wide in time (as the oscillator jumps to the other branch the total field is still decreasing and only after it settles there the pulse field envelope starts to decrease). This fact can be seen more clearly in Fig. 5. There we show the Poincaré map phase diagram of the fully numerical time evolution ($-+-$line) of the switching between the two stable modes. The other lines in this figure represent the results obtained from the AM calculations. We notice that as the pulses get longer there is a convergence toward the adiabatic result.

The switching between the stable branches of the bistability region of the Duffing oscillator can also alternatively be controlled with a frequency-modulated force as can be seen in Figs. 6 and 7. In those figures the underlying small and large stable orbits are still clearly noticed.

B. Non-Markovian dissipation

In Fig. 8 we show that noise in the Duffing equation with memory is only relevant inside the instability zones of Eq. (7). In particular the approximation taken in Eq. (8) is con-

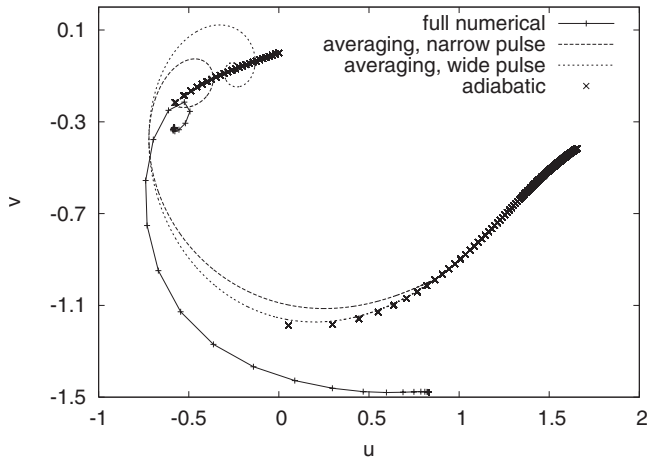

FIG. 5. Poincaré map of the time evolution of the Duffing oscillator given by Eq. (1) subjected to an ac drive plus a control pulse is given by the crossed line. The corresponding evolution given by the averaged system is shown in the dashed and dotted lines. The adiabatic limit is given by the X's.

sistent on average when the oscillator parameters are set outside of the instability zones. That approximation is usually good when the driving force is not large and the driving frequency is away from the strongest parametric resonance of Eq. (7).

We can see some fundamental differences between the usual linear damped oscillator and the non-Markovian damped oscillator in Fig. 9. In this figure we depict the response of five kinds of oscillators: nondissipative, Markovian, and non-Markovian (diffusive, subdiffusive, and superdiffusive) after an initial δ-function excitation. There is no external ac field applied here. In the Markovian case the frequency of the transient response is always smaller that the natural frequency ω_0 of the oscillator. We notice that the frequency of the transient responses of the three different non-Markovian dissipation regimes can be larger than ω_0. This is more markedly seen in the diffusive and subdiffusive responses as expected from Eqs. (16) and (17). This shift in the resonant frequency occurs due to a change in the effective mass of the oscillator and also on the restoring force of the oscillations due to the response of the fluid around the oscillator contained in the memory function. The parameters of the oscillators are indicated in the figure. The differences between the transient results of Fig. 10, in which the natural frequency is $\omega_0^2=0.5$, are more pronounced than in Fig. 9, in which $\omega_0^2=1.0$. This occurs because the closer ω_0 becomes to zero, bringing along also the resonant frequency ω_R, the more relevant the differences in response between the dissipation regimes become [since in diffusion $0<\tilde{\Gamma}(i\omega)<\infty$, in subdiffusion $\tilde{\Gamma}(i\omega)\to\infty$, and in superdiffusion $\tilde{\Gamma}(i\omega)\to 0$ as $\omega\to 0$]. This information could lead to simple transient-oscillation experiments with NEMS to test whether they are

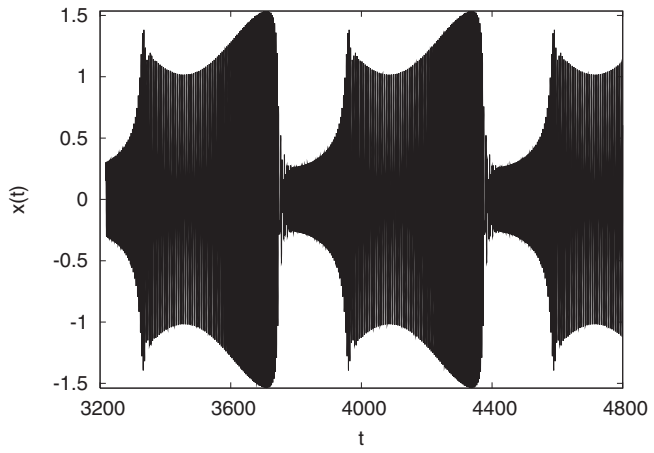

FIG. 6. A time series of the evolution of $x(t)$ when the Duffing oscillator is driven by a force with frequency modulation given by $\omega(t)=\omega+\beta\cos(\nu t)$, where $\omega=1.43$, $\beta=0.29$, and $\nu=0.01$.

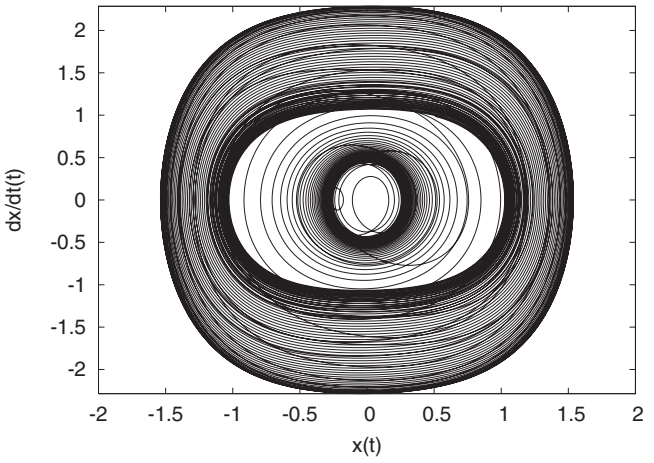

FIG. 7. One can see clearly the loop around the two stable periodic orbits as one cycles over the drive frequency. The accumulation curves indicate that the underlying features of the bistability region are still present when the Duffing oscillator is driven by a force with frequency modulation given by $\omega(t)=\omega+\beta\cos(\nu t)$, where $\omega=1.43$, $\beta=0.29$, and $\nu=0.01$.

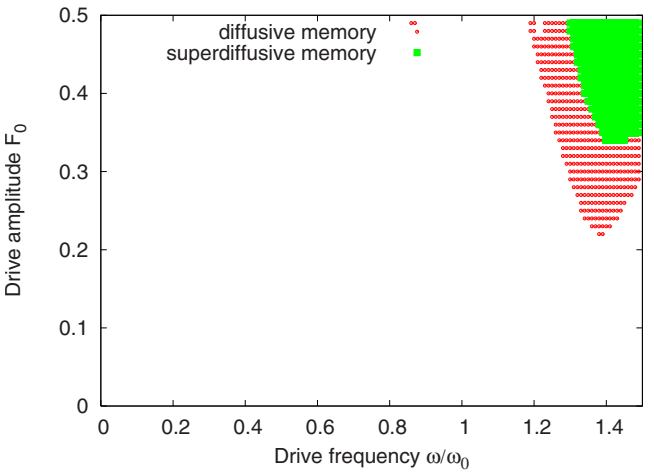

FIG. 8. (Color online) A numerical investigation of the instability zones of Eq. (7) is shown in the figure for oscillators with diffusive and superdiffusive memories. The parameters are given by $\alpha=1.0$, $\omega_0=1.0$ (for both oscillators); with $\Gamma_0=0.54$ and $\tau=1.0$ for the diffusive oscillator, and $\Gamma_0=0.8$, $\Gamma_1=0.4$, $\tau_0=1.0$, and $\tau_1=2.0$ for the superdiffusive oscillator.

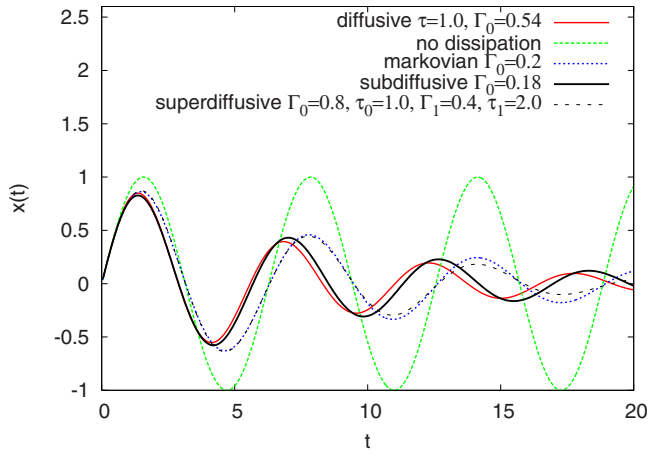

FIG. 9. (Color online) Comparison of the transients of a simple linear damped oscillator and of an oscillator with non-Markovian damping with the oscillations of the corresponding nondissipative oscillator. All oscillators in this figure are excited to the same initial conditions, then are left alone without external force to oscillate. The parameters of the oscillators are given by $\alpha=0.0$, $K_0=0.0$, $\omega_0=1.0$, and Γ_0's indicated in the figure. Note that the higher frequency of the non-Markovian oscillators is due to the response of the dissipative medium around the oscillator, which is taken into account by the memory function $\Gamma(t)$.

in the non-Markovian regime or not. In these experiments noise could be eliminated by adding up the results of many successive measurements.

Linear absorption line curves of the three dissipative processes are shown in Figs. 11 and 12. We choose different values of Γ_0 for each regime in such a way that their absorption peak values are approximately the same when $\omega_0^2=1.0$. Hence, the corresponding responses will be as close as possible for the same excitation. In Fig. 12 we see that these responses become markedly different because the memory functions are very distinct near $\omega=0$. In this figure we have a

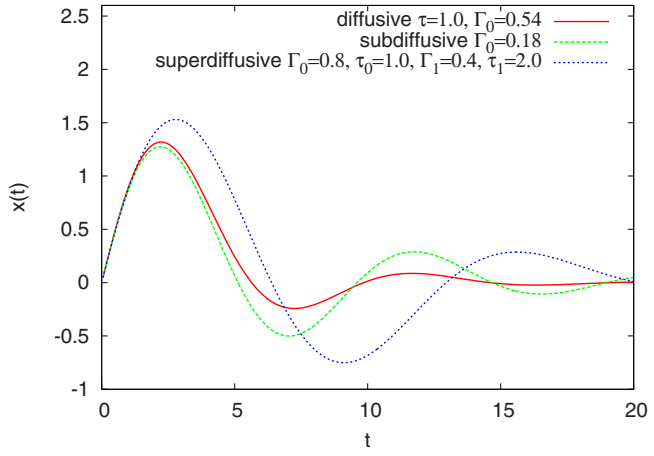

FIG. 10. (Color online) Comparison of the transients of oscillators with the three regimes of non-Markovian damping. All oscillators in this figure are excited to the same initial conditions, then are left alone without external force to oscillate. The parameters of the oscillators are given by $\alpha=0.0$, $K_0=0.0$, $\omega_0=0.5$, and the Γ_0's are indicated in the figure.

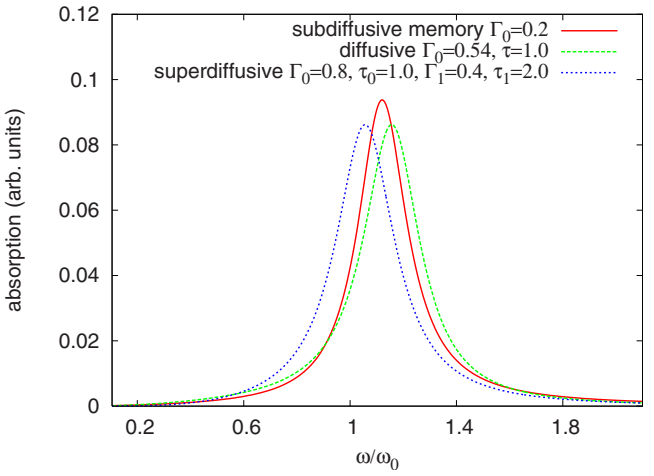

FIG. 11. (Color online) Linear response. Absorption lines for the three regimes of non-Markovian dissipation when the natural frequency is $\omega_0=1.0$ and $\alpha=0$.

log-log plot of the absorption lines for the three regimes of non-Markovian dissipation. The power law behavior is clearly seen in the slope of the absorption lines in the log-log plot. By measuring the slopes we obtain the power laws $P(\omega)\propto\omega^{\nu}$, where $\nu<2$ for subdiffusion, $\nu=2$ for diffusion, and $\nu=4$ for superdifusion.

Absorption line curves with hysteresis for the Duffing oscillator with diffusive memory are presented in Fig. 13. These results are obtained from the full numerical integration of Eq. (15). The parameters used are $\alpha=1.0$ and $\omega=1.43$. A range of values for Γ_0 and τ are used in such a way that $\Gamma_0\tau=0.2$. We then use shorter and shorter values of τ. In the limit $\tau\to 0$ we obtain the corresponding response of the usual Duffing oscillator without memory as expected. We show a comparison of numerical and analytical absorption-line curves with hysteresis for the Duffing oscillator with memory in Fig. 14. Only the stable branches are shown in the numerical absorption curve, while the AM theoretical

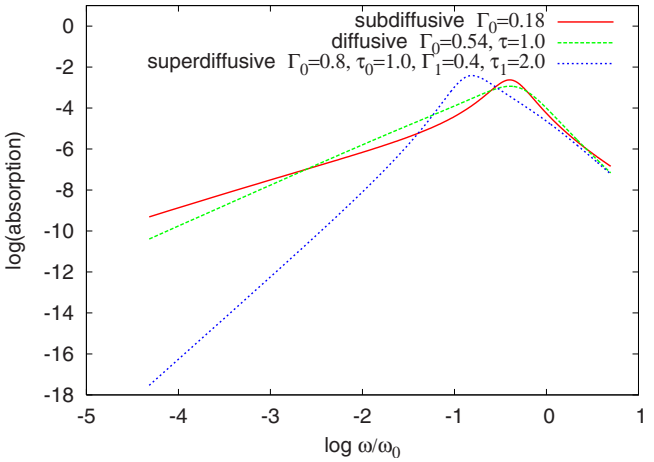

FIG. 12. (Color online) Linear response. log-log plot of the absorption lines for the three regimes of non-Markovian dissipation when the natural frequency is $\omega_0=0.5$ and $\alpha=0$. The power law behavior is clearly seen in the lines above as ω^{ν}, with $\nu<2$ for subdiffusion, $\nu=2$ for diffusion, and $\nu=4$ for superdiffusion.

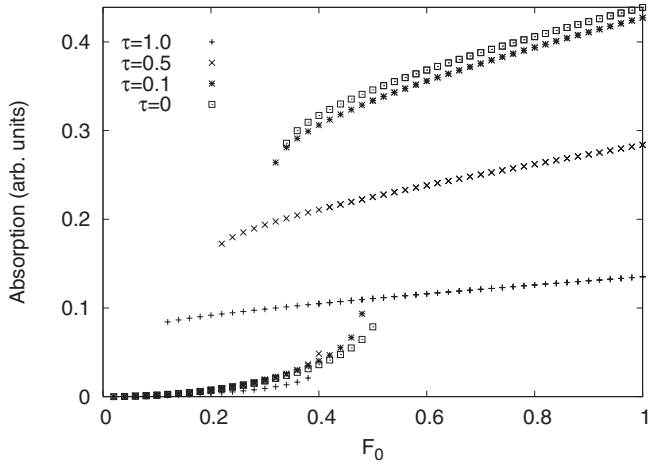

FIG. 13. Absorption-line curves with hysteresis for the Duffing oscillators with memory (only the stable branches are shown). These results are obtained from the full numerical integration of Eq. (15). The parameters used are $\alpha=1.0$, $\omega_0=1.0$, and $\omega=1.43$. A range of values for Γ_0 and τ are used in such a way that $\Gamma_0\tau=0.2$. We then use shorter and shorter values of τ. In the limit $\tau\rightarrow 0$ we obtain the corresponding response of the usual Duffing oscillator without memory.

curve shows all three branches. The parameters are given by $\alpha=1.0$, $\Gamma_0=0.4$, $\tau=0.5$, and $\omega=1.43$. These results are included here only as consistency checks, first verifying that the Markovian limit is obtained once shorter and shorter correlation times are taken for the memory function and second that AM works well for the integrodifferential equations of motion of the non-Markovian oscillator. The extension of the bistable region is something that could be readily measured experimentally, what could serve as another test for the model provided the amount of noise is small. With the presence of noise we expect that these bistable regions shrink in a similar way as that observed by Aldridge and Cleland [8].

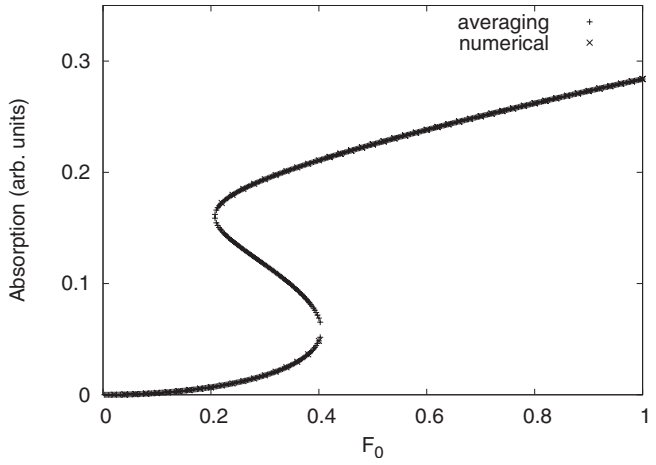

FIG. 14. Absorption-line curves for the Duffing oscillator with memory. Only the stable branches are shown in the numerical absorption curve, while the AM theoretical curve shows all three branches. The parameters are given by $\alpha=1.0$, $\Gamma_0=0.4$, $\tau=0.5$, $\omega_0=1.0$, and $\omega=1.43$.

V. CONCLUSIONS AND OUTLOOK

We have shown that bistability can be controlled in Duffing oscillators by in-phase or out-of-phase force-amplitude pulses, or by frequency-modulated driving. In the case of control via force-amplitude pulses, the envelope should vary adiabatically so that the control method is efficient and the AM (which is equivalent to the slowly varying envelope approximation) is applicable. The necessary peak fields for effectively controlling the stable responses were obtained from AM calculations. We performed this control approach in the ac-driven Duffing oscillator with Markovian dissipation. In the case of control via frequency modulation, we found that if the frequency varies adiabatically and its amplitude is large enough we can easily switch around the hysteretic loop.

We also investigated the role of non-Markovian dissipation processes over the linear and nonlinear responses of the Duffing oscillator to ac and δ-function excitations. We found both qualitative as well as quantitative differences in the responses of the non-Markovian oscillator as compared with the equivalent responses of the usual Markovian oscillator to the same excitation. The frequency of the transient response to a δ– function kick can be blueshifted with respect to the natural frequency, as opposed to the usual damped oscillator response, when it is always redshifted; a fact that could be explored in a simple experiment with NEMS to verify whether the oscillator is in the non-Markovian regime or not. Further information about the memory function could be obtained from the Fourier transform of the time evolution of $x(t)$. In fact, accurate measurement of $\tilde{\Gamma}(i\omega)$ could be obtained from linear response to either a δ-function kick, based on Eq. (9), or to steady-state ac driving, based on Eq. (11). For the ac-driven oscillator the amplitude and phase of the oscillations should be known for each driving frequency (or at least around resonance) for the memory function to be accurately determined from Eq. (11) except for intrinsic random noise deviations, which could be minimized by summing up the results of repeated experiments. Hence, one realizes that the sampling of the linear response $x(t)$ to a δ kick would give all the information necessary to find the memory $\Gamma(t)$ in a single experiment instead of the required sweep in the driving frequency for the ac-driven oscillator. We have investigated three different types of memory function, one for each type of Brownian motion: diffusive, subdiffusive, and superdiffusive. We found that each new time scale introduced in the dissipative process will create a new dimension in the dynamical system. We found further that in diffusive dissipation the average power absorbed near $\omega=0$ is given by $\lim_{\omega\rightarrow 0} P(\omega)\propto\omega^2$. This is a universal power law for oscillators with diffusive memory. We found that in subdiffusive dissipation the average power absorbed near $\omega=0$ is $\propto\omega^{3/2}$. Although, the exact exponent of the absorption may vary for different subdiffusive processes, this exponent has to be less than 2 for all subdiffusive processes. For superdiffusive dissipation the average power absorbed near $\omega=0$ is given by $\lim_{\omega\rightarrow 0} P(\omega)\propto\omega^4$. In general the exponent of the absorption for superdiffusive processes goes as ω^ν for $\omega\rightarrow 0$, where $\nu>2$. All these results are independent of nonlinear effects according to Eq. (14).

This study may be helpful in guiding future developments in NEMS science and technology. The control mechanisms proposed here can be applied to controlling bistability in NEMS, such as eliminating phase shifts generated by noise-induced jumps between the stable branches. Another possible technological application of the oscillating NEMS is related to the generation of microwave radiation through third-harmonic generation. In this case, the switching between the two stable responses can lead to any sequence of high and low third-harmonic generation, what could be used as a microwave modulator. Furthermore, the control mechanisms proposed here could be readily applied to other systems that present bistability such as intersubband transitions in quantum wells [21] and microcavities with optomechanical instabilities [22,23]. As the size of NEMS become smaller with increasingly higher fundamental-mode frequencies, memory effects will play an important role in the dynamics. This will be of paramount importance when NEMS are immersed in a fluid, since the fluid response changes significantly from low to high frequencies (when the fluid becomes viscoelastic). Finally, some fundamental theories about the role of memory in diffusion processes in fluids [12] could be tested by the proposed method of measurement of the memory function that could lead to a better understanding of Brownian motion.

[1] J. Guckenheimer and P. Holmes, *Nonlinear Oscillations, Dynamical Systems, and Bifurcations of Vector Fields* (Springer-Verlag, New York, 1983).
[2] A. H. Nayfeh and D. T. Mook, *Nonlinear Oscillations* (Wiley, New York, 1979).
[3] P. E. de Brito, J. A. Gonzalez, and H. N. Nazareno, Phys. Rev. B **54**, 12820 (1996).
[4] M. I. Dykman, D. G. Luchinsky, R. Mannella, P. V. E. McClintock, N. D. Stein, and N. G. Stocks, Phys. Rev. E **49**, 1198 (1994).
[5] G. Gabrielse, H. Dehmelt, and W. Kells, Phys. Rev. Lett. **54**, 537 (1985).
[6] I. Siddiqi, R. Vijay, F. Pierre, C. M. Wilson, M. Metcalfe, C. Rigetti, L. Frunzio, and M. H. Devoret, Phys. Rev. Lett. **93**, 207002 (2004).
[7] B. Yurke, D. S. Greywall, A. N. Pargellis, and P. A. Busch, Phys. Rev. A **51**, 4211 (1995).
[8] J. S. Aldridge and A. N. Cleland, Phys. Rev. Lett. **94**, 156403 (2005).
[9] A. Erbe, H. Krommer, A. Kraus, R. H. Blick, G. Corso, and K. Richter, Appl. Phys. Lett. **77**, 3102 (2000).
[10] M. C. Cross, A. Zumdieck, R. Lifshitz, and J. L. Rogers, Phys. Rev. Lett. **93**, 224101 (2004).
[11] R. Almog, S. Zaitsev, O. Shtempluck, and E. Buks, Appl. Phys. Lett. **88**, 213509 (2006).
[12] R. Morgado, F. A. Oliveira, G. G. Batrouni, and A. Hansen, Phys. Rev. Lett. **89**, 100601 (2002).
[13] M. Grifoni and P. Hänggi, Phys. Rep. **304**, 229 (1998).
[14] H. B. Peng, C. W. Chang, S. Aloni, T. D. Yuzvinsky, and A. Zettl, Phys. Rev. Lett. **97**, 087203 (2006).
[15] J. P. Hansen and I. R. McDonald, *Theory of Simple Liquids* (Academic, New York, 1976).
[16] S. Kim and K. Kihm, Appl. Phys. Lett. **90**, 081908 (2007).
[17] G. Suire and G. Cederbaum, Int. J. Mech. Sci. **37**, 753 (1995).
[18] J. A. Sanders and F. Verhulst, *Averaging Methods in Nonlinear Dynamical Systems* (Springer-Verlag, Berlin, 1985).
[19] M. I. Dykman and M. A. Krivoglaz, Sov. Phys. JETP **50**, 30 (1979).
[20] V. I. Arnold, *Ordinary Differential Equations* (MIT, Cambridge, 1995), p. 205.
[21] H. O. Wijewardane and C. A. Ullrich, Appl. Phys. Lett. **84**, 3984 (2004).
[22] A. Dorsel, J. D. McCullen, P. Meystre, E. Vignes, and H. Walther, Phys. Rev. Lett. **51**, 1550 (1983).
[23] O. Arcizet, P.-F. Cohadon, T. Briant, M. Pinard, and A. Heidmann, Nature (London) **444**, 71 (2006).